

“Effect of change in strain path during cold rolling on the evolution of microstructure, texture and hardness properties of nickel with extremely coarse initial grain size”

Vijay Prakash Chaudhary

A Dissertation Submitted to
Indian Institute of Technology Hyderabad
In Partial Fulfillment of the Requirements for
The Degree of Master of Technology



भारतीय प्रौद्योगिकी संस्थान हैदराबाद
Indian Institute of Technology Hyderabad

Department of Material Science & Engineering

June 2012

Declaration

I declare that this written submission represents my ideas in my own words, and where others' ideas or words have been included, I have adequately cited and referenced the original sources. I also declare that I have adhered to all principles of academic honesty and integrity and have not misrepresented or fabricated or falsified any idea/data/fact/source in my submission. I understand that any violation of the above will be a cause for disciplinary action by the Institute and can also evoke penal action from the sources that have thus not been properly cited, or from whom proper permission has not been taken when needed.

Prakash

Vijay Prakash Chaudhary

Roll No: ms10m02

Approval Sheet

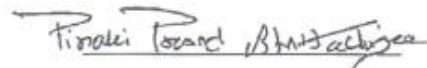
This thesis entitled “Effect of change in strain path during cold rolling on the evolution of microstructure, texture and hardness properties of nickel with extremely coarse initial grain size” by Vijay Prakash Chaudhary is approved for the degree of Master of Technology from IIT Hyderabad.



Dr. R. Ranjith (Department of Materials Science and Engineering), Examiner




Dr. Atul Deshpande (Department of Materials Science and Engineering), Examiner



Dr. Pinaki Prasad Bhattacharjee (Department of Materials Science and Engineering),

Thesis Supervisor



Dr. S. Surya Kumar (Department of Mechanical Engineering),

Chairman

Acknowledgments

I take this opportunity to express a deep sense of gratitude towards my thesis guide **Dr. Pinaki Prasad Bhattacharjee**, H.O.D, Department of Material Science & Engineering, for providing excellent guidance, encouragement and inspiration throughout the research work. Without his invaluable guidance, this work would never have been a successful one. I also want to thank **Professor U.B Desai**, Director, IIT Hyderabad for kindly allowing me to perform experimental work in IIT Bombay.

I would like to thank **Professor N. Tsuji**, Kyoto University, Japan for his kind permission to carry out the rolling of the specimens and **Professor I. Samajdar**, IIT Bombay, India, for allowing me to perform characterization of the deformed materials.

I would also like to thank all my friends at IIT Hyderabad for their valuable suggestions, helpful discussions and for making my stay in the institute campus a pleasure. I want to thank Ph. D scholars **Mr. J. R. Gatti** and **Mr. M. Z. Ahmed** for their co-operation in my experimental work. I want to specially thank my M. Tech. batchmate **Mr. Mohit Joshi** for his support, stimulating discussions and assistance throughout the course of this work.

I want to acknowledge my mother **Smt. Kamalawati Devi** and my brother **Mr. R. P. Chaudhary** for their blessings and moral support.

Finally I wish to express my deep sense of gratitude to everyone who helped me in completing the research work.

Vijay Prakash Chaudhary

Dedicated to

My mother

Smt. Kamalawati Devi

Abstract

The effect of strain path change during cold rolling on the evolution of microstructure, texture and hardness properties of high purity nickel (~99.7%) with extremely coarse starting grain size (~800 μm) has been studied in the present work. For this purpose two different rolling routes, namely, unidirectional cold rolling (UCR) and cross cold rolling (CCR) are investigated in the present work. The rolling direction is kept constant throughout the deformation process in UCR route but during CCR processing the rolling direction and the transverse direction are mutually interchanged in every consecutive pass by rotating the material around the normal direction. Nickel sheets were deformed up to 90% reduction in thickness using the two processing routes.

UCR processing route results in a microstructure having both lamellar and highly fragmented regions and pure metal or copper type deformation texture having strong presence of S, Cu and Bs orientations. The CCR processed microstructure also appears to be fragmented and locally sheared regions could be easily identified. The texture of CCR processed material is characterized by strong presence of the S component. The two processing routes are found to affect the hardness properties significantly. The hardness of UCR processed materials increases with increasing thickness reduction due to cold rolling which may be explained by the usual strain-hardening behavior. In contrast, the hardness of CCR processed material increases up to 65% deformation and thereafter it is found to decrease.

A comparison of the present observations with the texture evolution in conventional grain sized material reveals that UCR processing irrespective of grain size results in similar deformation texture in both conventional and coarse grain sized materials. On the other hand, starting grain size has a very strong effect on the evolution of texture during CCR processing. Local shearing observed in the microstructure of CCR processed coarse grained material is thought to play an important role by way of fragmentation of structure and rotation of crystals into different orientations resulting in different texture evolution than its conventional grained counterpart. The structure-property relationship in CCR processed coarse grained nickel is, however, required to be studied in more detail to clarify the observed differences in the evolution of hardness properties due to two processing routes.

Nomenclature

CGSM- Coarse Grain Sized Material

UCR- Unidirectional Cold Rolling

CCR- Cross Cold Rolling

SCR- Straight Cold Rolling

GO map- Grain Orientation map

GB map- Grain Boundary map

ODF- Orientation Distribution Function

PF- Pole Figure

FCC- Face Centered Cubic

SFE- Stacking Fault Energy

RD- Rolling Direction

TD- Transverse Direction

ND- Normal Direction

HAGB- High Angle Grain Boundary

LAGB- Low Angle Grain Boundary

XRD- X Ray Diffraction

EBSD- Electron Back Scattered Diffraction

VH- Vickers Hardness

Contents

Declaration.....	ii
Approval Sheet.....	iii
Acknowledgements.....	iv
Abstract.....	v
Nomenclature.....	vii
1 Introduction.....	1
2 Literature Review.....	3
2.1 Objective & scope.....	5
3 Experimental Procedure.....	6
3.1 Preparation of starting material.....	6
3.2 Deformation processing.....	7
3.3 Characterization.....	8
3.3.1 Sample preparation.....	8
3.3.2 Microstructural & textural characterization.....	9
3.3.3 Microindentation hardness testing.....	9
4 Experimental Results.....	11
4.1 Starting material.....	11
4.2 Deformation by UCR.....	14
4.3 Deformation by CCR.....	22
4.4 Evolution of mechanical properties.....	28
5 Discussion.....	29
6 Summary & Conclusions.....	33
References.....	34

Chapter 1

Introduction

Deformation processing of metallic materials leads to changes in microstructures and crystallographic textures which may be related to the characteristic deformation behavior of different metallic systems. The development of microstructures and textures, in general, depend on several processing parameters such as temperature, strain, strain rate and strain path. In case of metals and alloys the strain path change has important effects on the evolution of microstructure and texture [1, 2] and consequently may significantly affect the end properties of materials.

For deformation under rolling geometry the effect of strain path change can be studied easily by changing the rolling and transverse direction (RD and TD, respectively as shown in Fig. 1.1). Generally, strain path change in rolling is achieved by using two different types of rolling routes named as unidirectional cold rolling (UCR) & cross cold rolling (CCR). In straight cold rolling the rolling direction (RD) is kept constant throughout the deformation process whereas in the cross cold rolling sample is rotated by 90° around normal direction (ND) so that the TD of previous rolling pass will become rolling direction of current rolling pass.

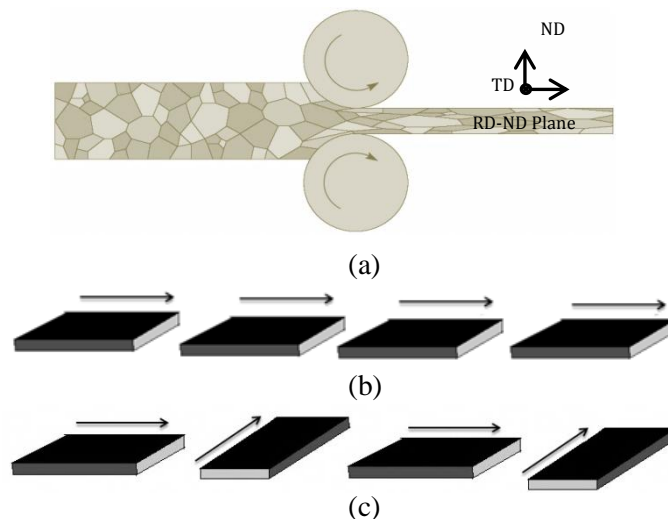


Figure 1.1: (a) Description of reference directions, RD- Rolling Direction, ND-Normal Direction and TD- Transverse Direction and RD-ND plane in rolling, (b) Unidirectional cold rolling (UCR) (c) Cross cold rolling (CCR). Black arrow represents rolling direction of first pass with its orientation.

The objective of present research work is to investigate the strain path effect on microstructural and textural evolution during heavy cold rolling of high purity Nickel (99.7% purity) with very coarse starting grain size of $\sim 800 \mu\text{m}$. For this study two set of samples deformed by two different rolling routes, namely, UCR and CCR up to 90% reduction in thickness and detailed microstructural and mechanical property characterization has been done at different length scales using X-ray, electron back scatter diffraction techniques (XRD and EBSD, respectively) and hardness testing. Finally, the results obtained are also compared with conventional grain sized starting material (average grain size of $\sim 36 \mu\text{m}$ which has been investigated in a parallel study) to clearly elucidate the effect of starting grain size.

Chapter 2

Literature Review

A substantial research work has been conducted to study the evolution of microstructure and texture in a face centered cubic (FCC) materials during rolling [2-6]. The development of lamella structure with increasing strain is very commonly observed in heavily rolled materials. This microstructural changes are accompanied by the development of crystallographic texture. For FCC materials the rolling texture is usually characterized by the two incomplete fiber textures, α -fiber and β -fiber as shown in Fig. 2.1 α -fiber which extends from Goss orientation ($\{110\} \langle 001 \rangle$) to brass orientation ($\{110\} \langle 112 \rangle$) and β -fiber which extends from copper orientation (Cu component; $\{112\} \langle 111 \rangle$) to brass orientation through S-orientation ($\{123\} \langle 634 \rangle$) [4]. In high to medium stacking fault energy (SFE) FCC materials like Al, Ni the deformation texture is characterized by pure metal type texture which has the presence of Cu, S and Brass components whereas in low SFE materials deformation has brass texture as characteristic.

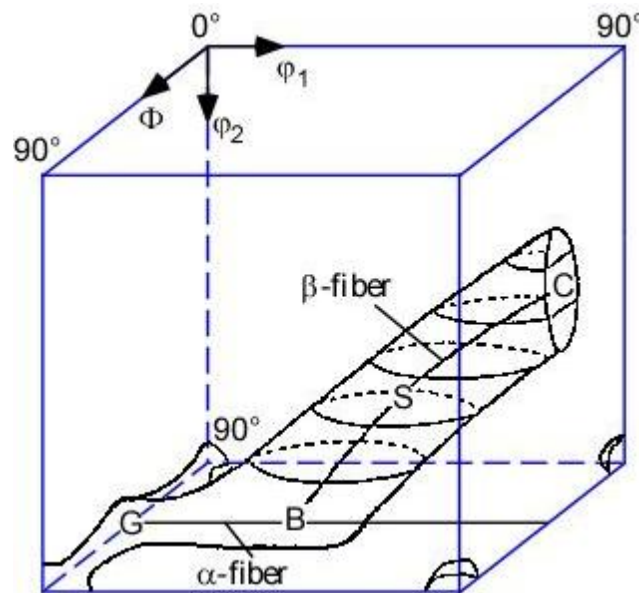


Figure 2.1: FCC Material standard rolling texture with two characteristic fibres, β -fibre extends from Cu to Brass orientation through S orientation and α -fibre extends from Goss in Euler space [4].

The microstructure and texture of deformed FCC materials depends on dislocation substructures and stable orientations formed during deformation process [2, 6] and deviation from the above simplistic description of texture is frequently observed depending on the processing variables including starting grain size and strain path. The deformation microstructure and texture development is very sensitive to strain path change [7]. In UCR route the rolling texture strengthen with strain whereas during CCR processing the substructures are rotated by 90^0 which make stable orientations and substructure of previous pass unstable along new rolling direction. Limited research work is available indicate that CCR processed microstructure and texture differ considerably from those of UCR. Figure 2.2 shows the characteristics differences in the textures developed in the two different processing routes. It has been generally observed that brass and rotated brass components develop in CCR processed conventional grain sized copper and nickel [7, 10].

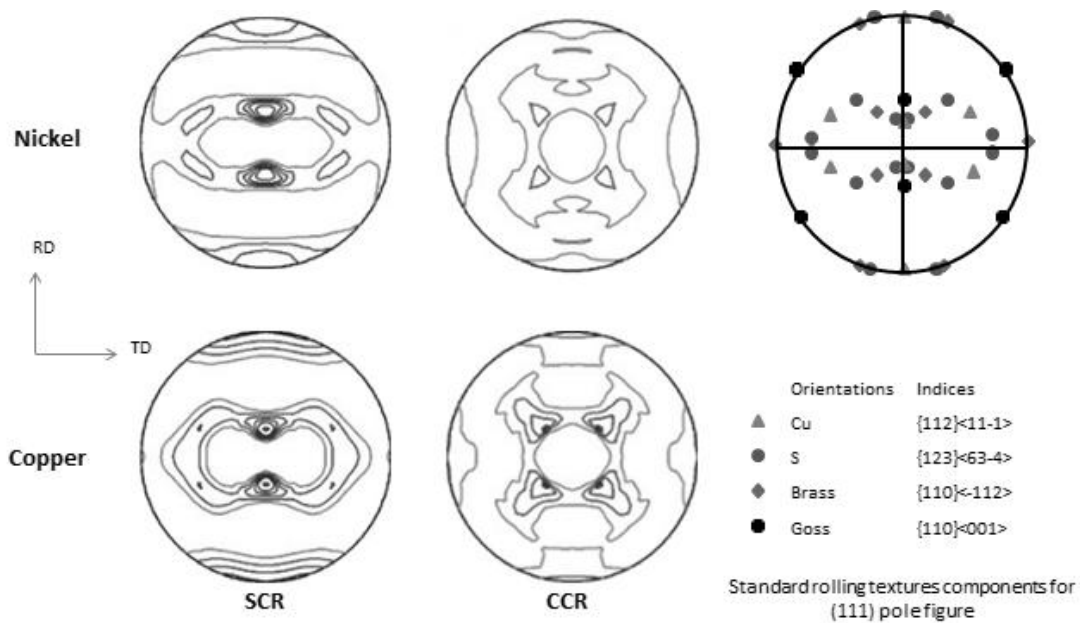


Figure 2.2: (111) pole figures of nickel and copper deformed by UCR and CCR routes [8].

While the effect of CCR process has been investigated in different metallic systems [7-10] almost all of the prior investigations have been conducted on conventional grain sized materials. Surprisingly the effect of CCR processing in very coarse grain sized materials is still largely unknown although it is well established that starting grain sized can have important consequences on deformation and recrystallization microstructure and texture development such as increased propensity for the formation of shear bands and suppression of cube recrystallization texture in very coarse grained starting materials

[1, 10-12]. In turn, the effect of starting grain size on different rolling routes also remains unclear. The motivation for the present study is to clarify these effects.

2.1 Objective & Scope

The objective of present research work is to investigate the strain path effect on microstructural and textural evolution during heavy cold rolling of high purity Nickel (99.7% purity) with very coarse starting grain size of $\sim 800\mu\text{m}$. For this study two set of samples deformed by two different rolling routes, namely, UCR and CCR up to 90% reduction in thickness and detailed microstructural and mechanical property characterization has been done at different length scales using X-ray, electron back scatter diffraction techniques (XRD and EBSD, respectively) and hardness testing. Finally, the results obtained are also compared with conventional grain sized starting material (average grain size of $\sim 36\ \mu\text{m}$ which has been investigated in a parallel study) to clearly elucidate the effect of starting grain size.

Chapter 3

Experimental Procedure

3.1 Preparation of Starting Material

Preparation of starting material (coarse grain starting material or CGSM) starts with the as-received Ni plate having dimension ($\sim 160\text{mm}^L \times 60\text{mm}^W \times 10\text{mm}^T$). The as-received plates were cold rolled up to 50% by multi-pass cold rolling on a laboratory scale rolling mill with well lubricated roll at room temperature followed by annealing at 1100°C for 1 hr in a salt bath furnace. Due to annealing, the rolled material fully recrystallized and extensive grain growth occurred resulting in very coarse grained starting material (CGSM). The processing stages are shown in a flow diagram in Fig. 3.1.

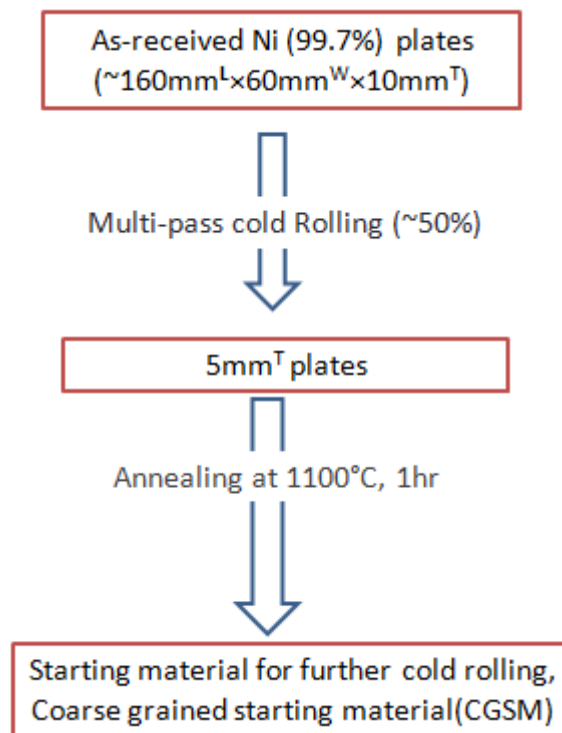


Fig.3.1: Flow chart for preparation of starting material (CGSM)

3.2 Deformation Processing

The starting material was deformed by two different routes, namely, unidirectional cold rolling (UCR) and Cross cold rolling (CCR). In the UCR route, the rolling direction (RD) was kept the same throughout the processing but in CCR route a 90° rotation about the normal direction (ND) was imparted between successive rolling passes as shown in Fig.3.2. The rolling process was performed on a laboratory scale rolling mill with well lubricated rolls at room temperature.

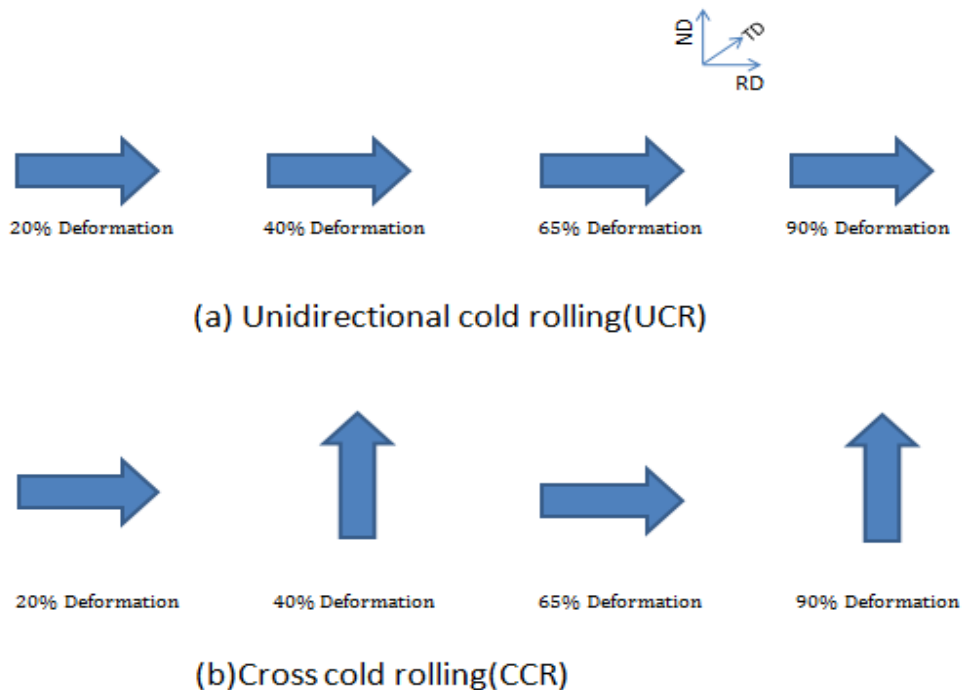


Fig.3.2 Description of (a) UCR and (b) CCR rolling routes

By both rolling routes we cold rolled the starting material to prepare 20%, 40%, 65%, 90% deformed samples to study the evolution of microstructure and texture as shown in fig.3.3.2.

3.3 Characterization

3.3.1 Sample preparation

There were three steps in sample preparation as listed below:

- (a) Cutting
- (b) Polishing (mechanical and automatic polishing)
- (c) Electropolishing

All rolled samples were first cut into small pieces using precision cutters Secotom-15 (Struers, Denmark) and Minitom, (Struers, Denmark) and marking the RD. After the cutting operation, these samples were mechanically polished. Firstly, the samples were polished using emery paper of coarse grit size (100) followed by fine grit size (1200). In the second stage, these samples were polished by using 3 μm (DiaDuoTM, Struers, Denmark) diamond solution in a manual polishing machine Labpol-5 (Struers, Denmark) followed by polishing using 1 μm colloidal silica in an automatic polishing machine Tegramin-25 (Struers, Denmark). For electron backscatter diffraction (EBSD) investigation, the mechanically polished samples were further electropolished using a solution of 90% methanol and 10% Perchloric acid as electrolyte. All polishing operations were carried out from the TD normal or RD-ND plane of rolled samples which was the plane under observation.

For microindentation hardness testing (microhardness testing), firstly the samples were mounted on a hot mounting press CitoPress -10 (Struers, Denmark) and then polished as described above. The hardness samples were mounted using a thermosetting resin (MultiFastTM, Struers, Denmark) such that the RD-ND plane is exposed out from the mounted specimen as shown in Fig. 3.3.1.



Fig.3.3.1- Mounted samples for hardness testing

3.3.2 Microstructural and Textural Characterization

Microstructural and textural characterizations of the prepared samples were done by X-ray (XRD) and EBSD techniques. Bulk texture analysis by XRD was carried out using a Panalytical MRD system using Cu-K_α radiation (1.54Å). Fully computer controlled EBSD system attached to a FEG-SEM (FEI, Quanta, 3D FEG) was used for microstructure and microtexture measurements. The EBSD scan data were analyzed using TSL-OIM™ software.

3.3.3 Microindentation Hardness Testing (Microhardness testing)

Microhardness test was performed on the RD-ND plane of the deformed samples to study the evolution of mechanical properties in different rolling routes (UCR and CCR) and compare their hardness properties. The hardness test was done using a load of 500 gm and dwell time of 10 sec. per indentation. To determine the average hardness value, five indentations were taken per sample and a gap of 250µm was maintained between successive indentations. These tests were carried out on microhardness testing equipment, DuraScan (EmcoTest™, Austria).

Fig. 3.3.2 summarizes the experimental work carried out in the present research work.

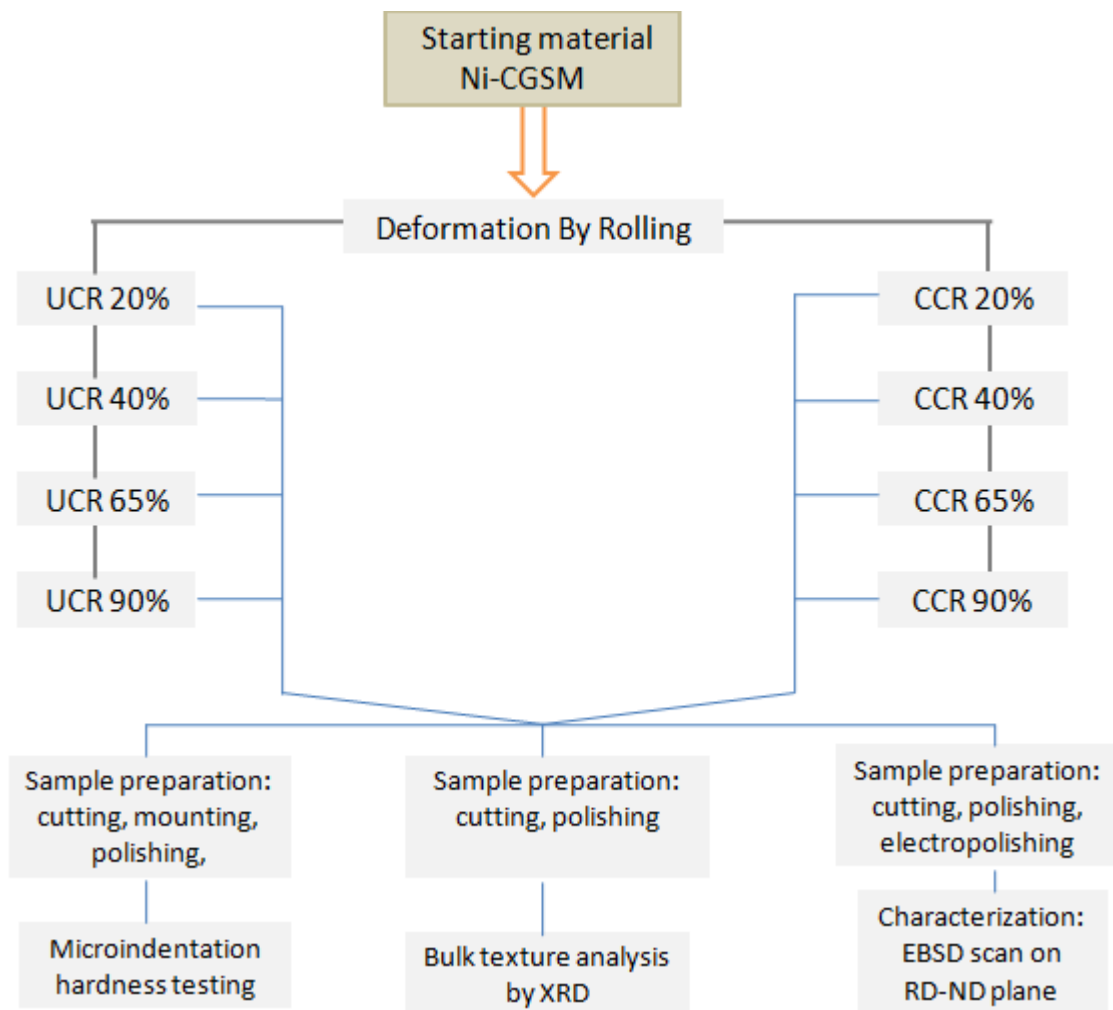


Fig.3.3.2- Flow chart showing the experimental work carried out in the present research work.

Chapter 4

Experimental Results

4.1 Starting Material

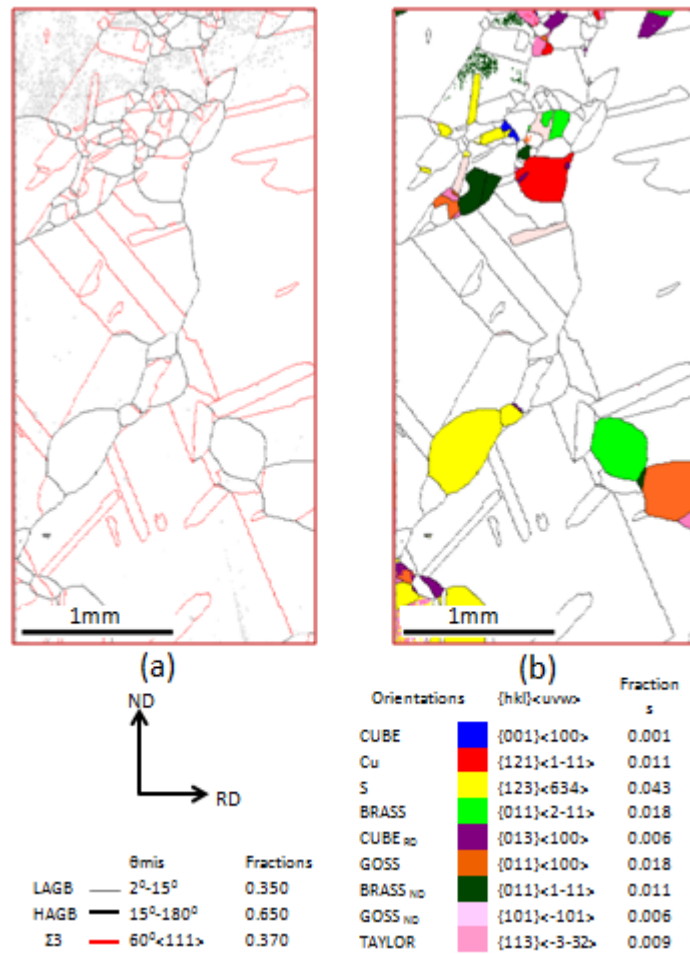


Fig.4.1.1: (a) Grain boundary and (b) orientation maps of the starting material.

Figure 4.1.1 (a) shows the Grain Boundary map (GB map) acquired from the RD-ND section of the Starting Material. The High Angle Grain Boundaries (HAGBs with misorientation angle (θ); $15^\circ \leq \theta \leq 180^\circ$) are highlighted in black lines while the grey lines represent the Low Angle Grain Boundaries (LAGBs with $15^\circ \geq \theta \geq 2^\circ$). The annealing twin boundaries ($\Sigma 3$ defined by $60^\circ\langle 111 \rangle$ relationship) have been highlighted in red (The above conventions regarding grain boundaries are followed in all subsequent maps furnished in this section). From the microstructure it is clear that the starting material is fully

recrystallized with very large grain size of $\sim 800 \mu\text{m}$. The GB map also shows the presence of very large annealing twins. Fig. 4.1.1(b) shows the corresponding grain orientation map (GO map) which shows the spatial distribution and volume fraction of different orientations or texture components. The typical texture components considered are summarized in Table 4.1. Evidently the CGSM possess very weak texture presumably due to low deformation ($\sim 50\%$ reduction in thickness) before annealing. This is also clearly evidenced from Fig.4.1.2 (a) and (b) which shows the (111) pole figure and $\Phi_2=0^\circ, 45^\circ$ and 65° sections of the ODF of the CGSM.

Table 4.1: Typical texture components considered during rolling of sheet materials

Orientation	{hkl}<uvw>	(ϕ_1, ϕ, ϕ_2)	Notation	Highlighting color
Cube	{001}<100>	($0^\circ, 0^\circ, 0^\circ$)	C	blue
Copper	{112}<111>	($90^\circ, 35^\circ, 45^\circ$)	Cu	red
S	{123}<634>	($59^\circ, 36.7^\circ, 63.4^\circ$)	S	yellow
Brass	{110}<112>	($35.3^\circ, 45^\circ, 0^\circ$)	Bs	green
Goss	{110}<001>	($45^\circ, 45^\circ, 0^\circ$)	G	orange
Rotated Cube	{013}<100>	($0^\circ, 19^\circ, 0^\circ$)	C_{RD}	purple
Rotated Brass	{011}<111>	($54.7^\circ, 45^\circ, 0^\circ$)	Bs^{ND}	Dark green
Rotated Goss	{101}<101>	($90^\circ, 45^\circ, 90^\circ$)	G_{ND}	Light pink
Taylor	{113}<332>	($90^\circ, 27^\circ, 45^\circ$)	T	Pink

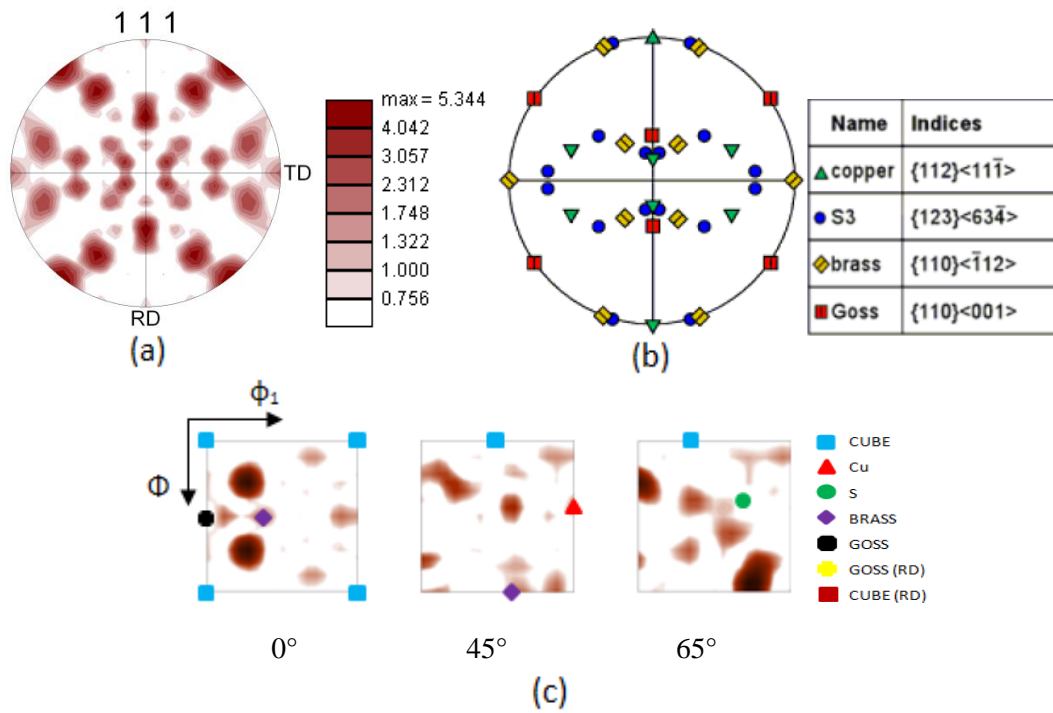


Fig.4.1.2: (a) Experimental (111) pole figure of the starting material and (b) is the (111) pole figure showing the ideal locations of the usual deformation texture components. (c) Shows the $\Phi_2=0^\circ, 45^\circ$ and 65° sections of the ODF of starting material.

4.2 Deformation by Unidirectional Cold Rolling (UCR)

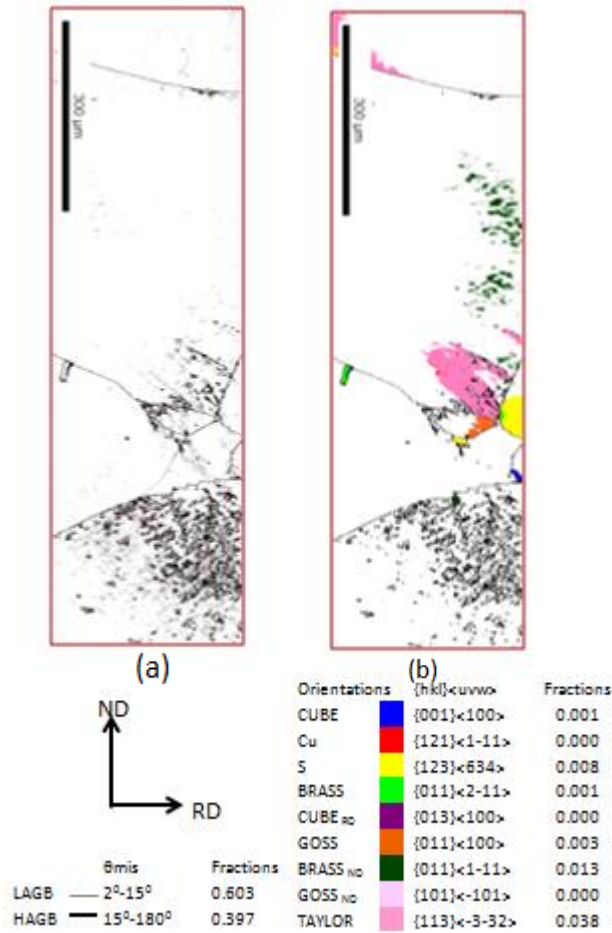


Fig.4.2.1- (a) Grain Boundary and (b) Grain Orientation maps of 20% UCR Material.

Figure 4.2.1(a) shows the GB map of the 20% deformed UCR processed material. The microstructure in this condition is still very coarse indicating the existence of the starting recrystallized grains. Inside the large grains, development of LAGB network could be observed. The corresponding GO map (Fig. 4.2.1(b)) shows very weak presence of (1 1 3) [-3 -3 2], (0 1 1) [1 -1 1] and (1 2 3) [6 3 -4] components along with very high fraction of random component.

Fig.4.2.2 (a) shows the (1 1 1) pole Figure of 20% UCR processed material. Comparison of this pole Figure with the standard (1 1 1) pole Figure of FCC crystal (Fig.4.2.2 (b)) shows weak presence of S and Bs components also evidenced in the GO map. This observation is also supported from the $\Phi_2=0^\circ, 45^\circ$ and 65° sections of Fig.4.2.2(c) of the ODF. These ODF sections show that there is absence of any dominant texture component in this condition.

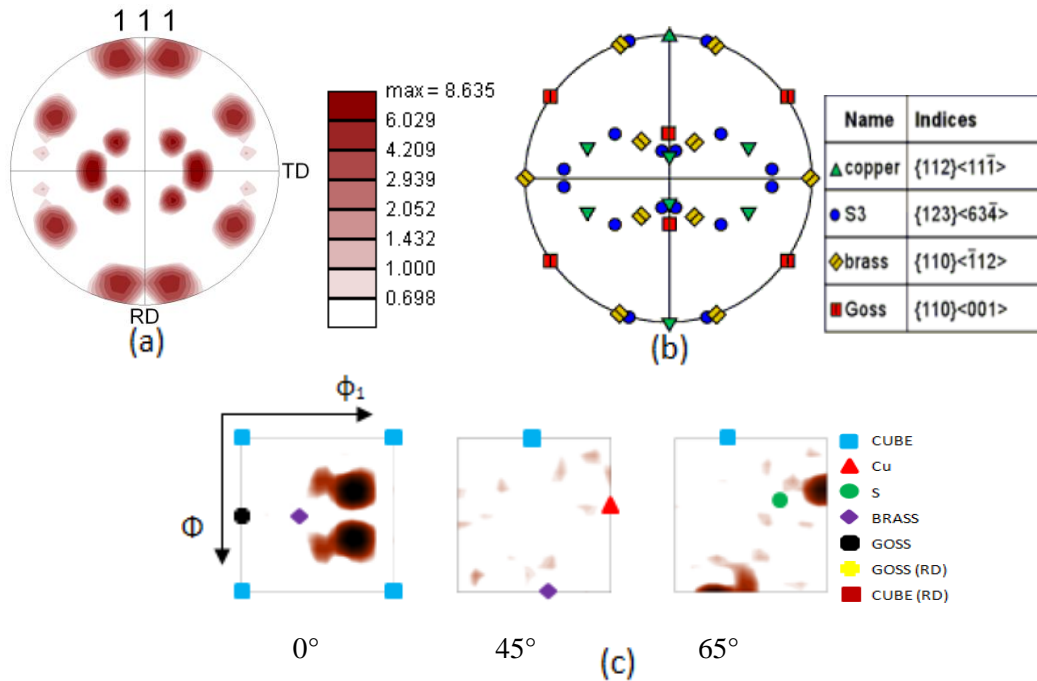


Fig.4.2.2: (a) (111) pole Figure of 20% UCR processed material and (b) is the standard (111) pole figure. (c) Shows the $\Phi_2=0^\circ$, 45° and 65° sections of the ODF.

After 40% deformation the LAGB network inside the grains becomes much more prominent as may be seen from the Fig.4.2.3 (a) which shows the GB map in this condition. It shows that the starting coarse microstructure still persists and the fraction of HAGBs (0.397 at 20% & 0.073 at 40% deformation) further decreases. Fig.4.2.3 (b) shows the corresponding GO map. The GO map reveals large S oriented region which appears to be fragment of an S oriented grain of the starting recrystallized material. The LAGBs network inside this grain is not very distinct compared to other deformed regions. The presence of isolated block of S oriented region is also reflected in the corresponding pole figure (Fig.4.2.4 (a)) and the $\Phi_2=0^\circ$, 45° and 65° sections (Fig.4.2.4 (c)).

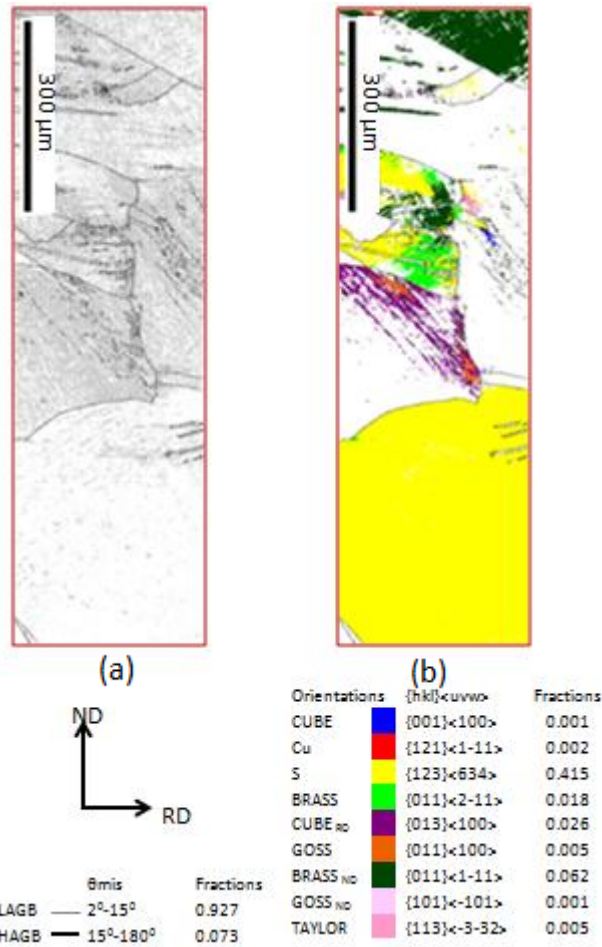


Fig.4.2.3: (a) GB and (b) GO maps of 40% UCR processed material.

Figure 4.2.4 (a) is the (111) pole Figure of 40% UCR material showing very weak Cu and Bs component and weak S component. Fig.4.2.4 (c) shows $\Phi_2=0^\circ, 45^\circ$ and 65° sections of the ODF of 40% UCR material. The $\Phi_2=0^\circ$ & 45° sections do not show any texture component and $\Phi_2=65^\circ$ shows weak S component.

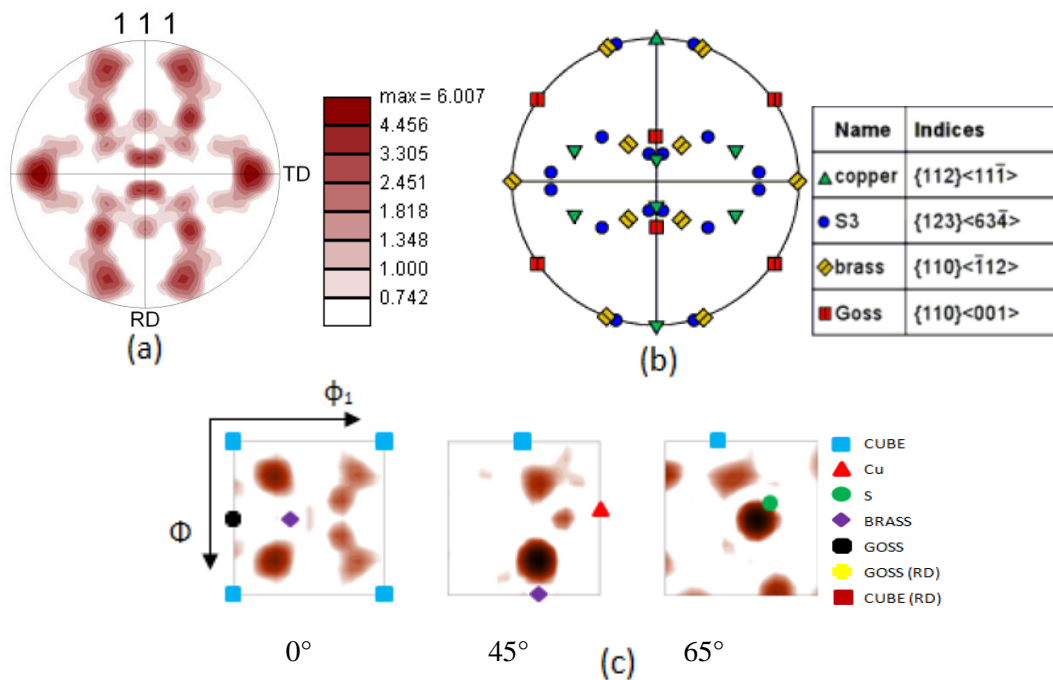


Fig.4.2.4: (a)-(111) pole Figure of 40% UCR processed material and (b)-the standard (111) pole figure. (c) Shows the $\Phi_2=0^\circ$, 45° and 65° sections of the ODF.

Figure 4.2.5 shows the microstructure and texture development following 65% deformation. Fig.4.2.5 (a) shows the GB map of 65% UCR processed material indicating the development of a banded microstructure, although, still very coarse and elongated along the RD. The GO map clearly indicates that different bands belong to different orientations. However, the two most prominent orientations in this deformed state are the B_S and S, having volume fraction of 0.218 & 0.370 respectively.

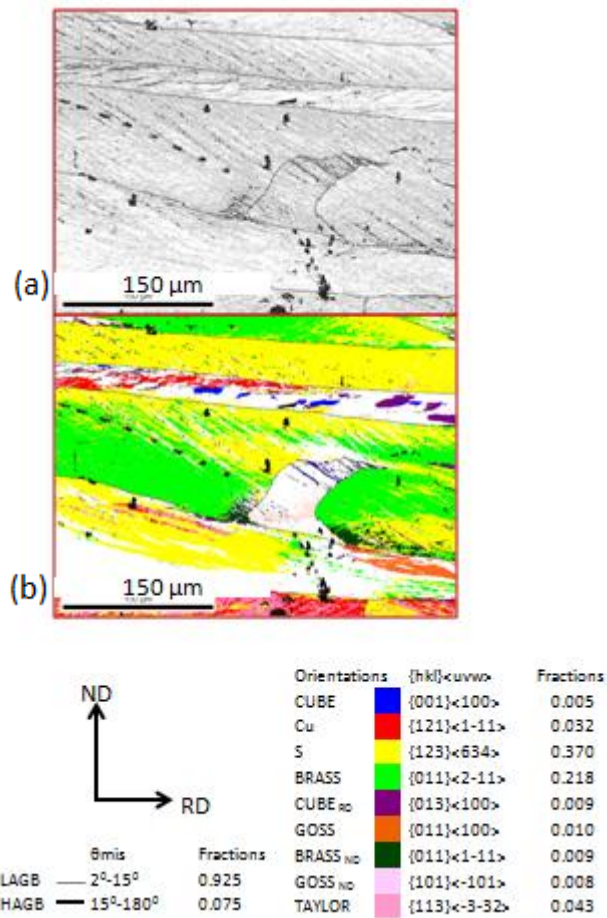


Fig.4.2.5: (a) GB and (b) GO maps of 65% UCR processed material.

The (111) Pole Figure of 65% UCR material (Fig.4.2.6 (a)) clearly shows the presence of strong S, Bs and G components. This is also clearly understood from the $\Phi_2=0^\circ, 45^\circ$ and 65° sections of the ODF of 65% UCR processed material (Fig.4.2.6(c)).

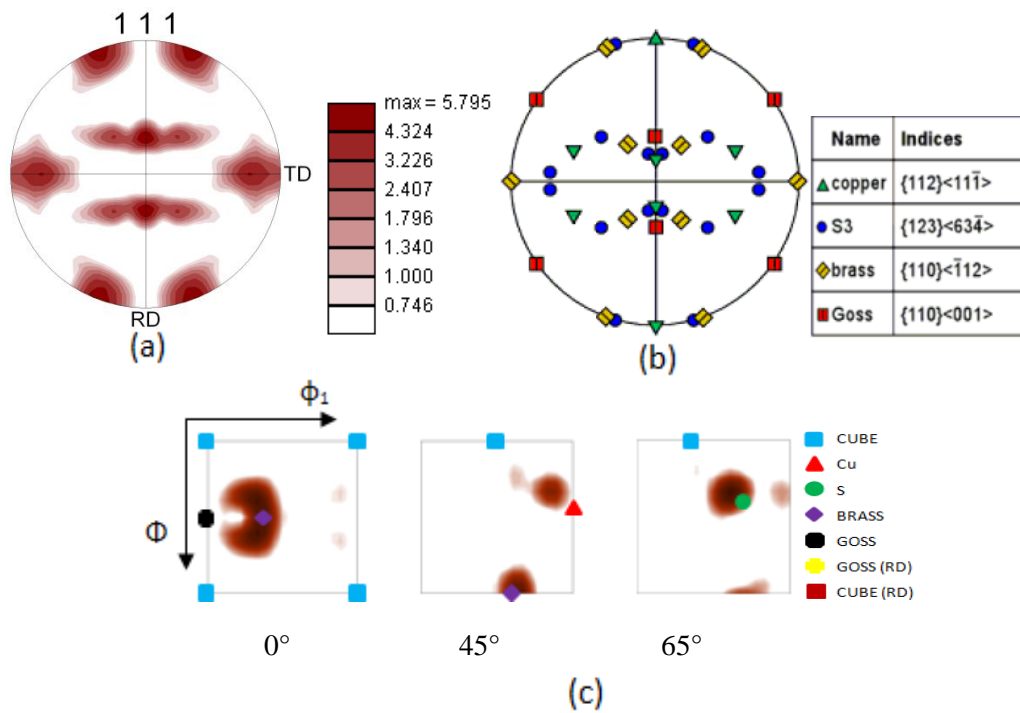


Fig.4.2.6: (a) (111) pole Figure of 65% UCR processed material, (b) is the ideal (111) pole figure. (c) Shows the $\Phi_2=0^\circ$, 45° and 65° sections of the ODF.

Figure 4.2.7(a) is the GB map of a region of interest in 90% UCR processed material showing a mixture of regions having more lamellar (shown in solid square) and fragmented (shown in broken square). The more lamellar regions show the presence of strong B_S and B_S^{ND} orientations while the fragmented regions show presence orientations G_{ND} orientation. Strong intensities at the $\Phi_2=0^\circ$ section of the ODF (Fig.4.2.8 (c)) around (90° , 45° , 0°) clearly reveals the presence of this component.

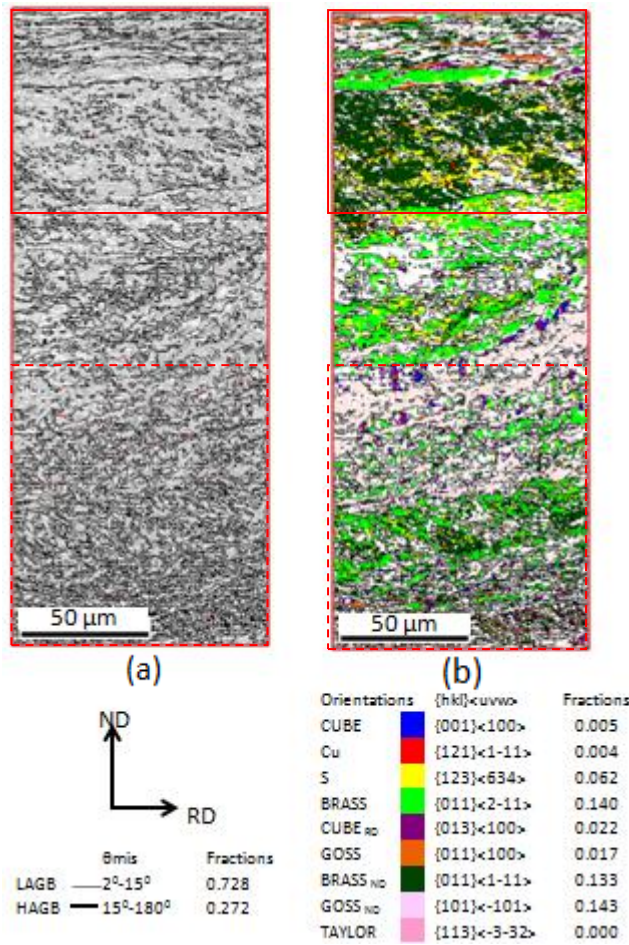


Fig.4.2.7: (a) GB and (b) GO maps of 90% UCR processed material.

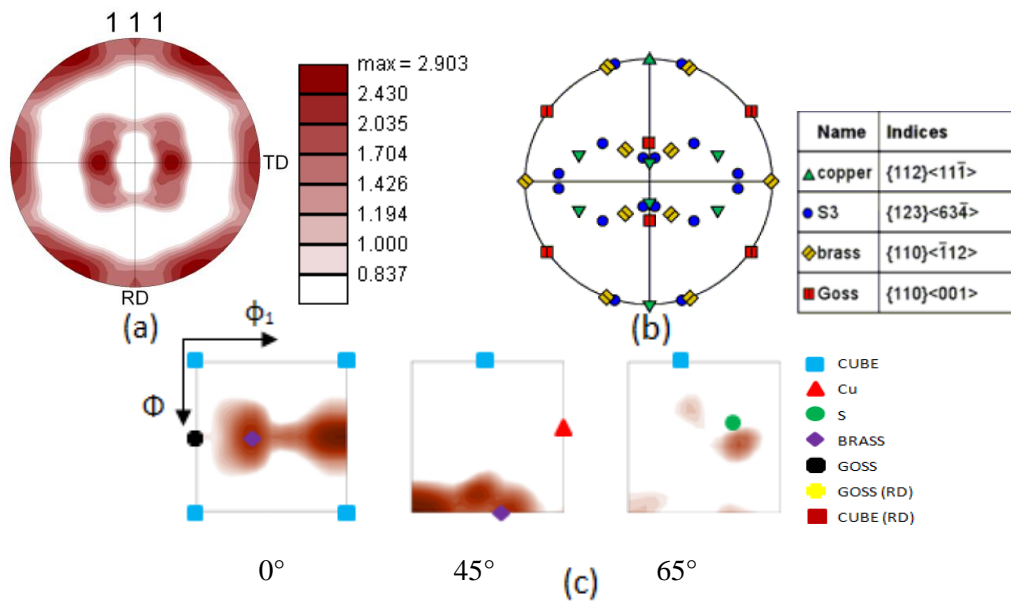


Fig.4.2.8 (a) Experimental (111) pole Figure of 90% UCR processed material and (b) is the ideal (111) pole figure; (c) shows the $\Phi_2=0^\circ, 45^\circ$ and 65° sections of the ODF.

The evolution of deformation texture by UCR processing has been further analysed by XRD. Fig.4.2.9 (a) and (b) shows the (111) pole figure & standard pole figure and (c) shows ODF, respectively; of the 90% UCR processed material. The pole figure appears typical of heavily cold rolled medium to high SFE materials indicating the development of a pure metal or copper type deformation texture. This is amply corroborated from the $\Phi_2=0^\circ, 45^\circ$ and 65° sections of the ODF which clearly indicates the presence of B_s, S and Cu components in the deformed material. Thus the bulk texture results appear somewhat different from the microtexture as far as the presence of S and Cu orientations are concerned.

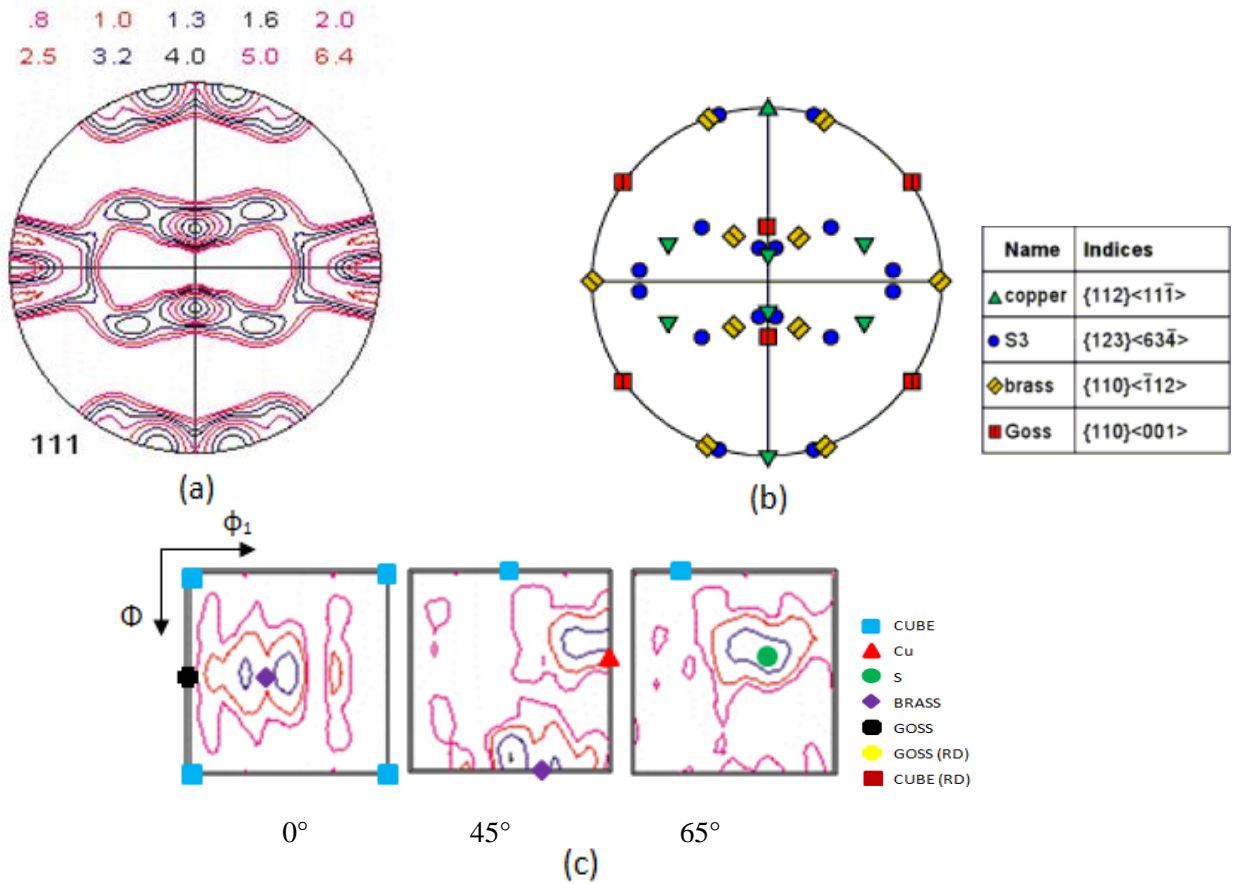


Fig.4.2.9: (a) Experimental (111) pole Figure of 90% UCR processed material and (b) is the ideal (111) pole figure; (c) shows the $\Phi_2=0^\circ, 45^\circ$ and 65° sections of the ODF. All measurements are obtained by XRD.

4.3 Deformation by Cross Cold Rolling (CCR)

The results of 20% CCR sample was very similar to the 20% UCR processed sample as deformation is carried out up to the same deformation level and along the same direction. Hence, the microstructures and textures in this deformed condition are not shown here separately.

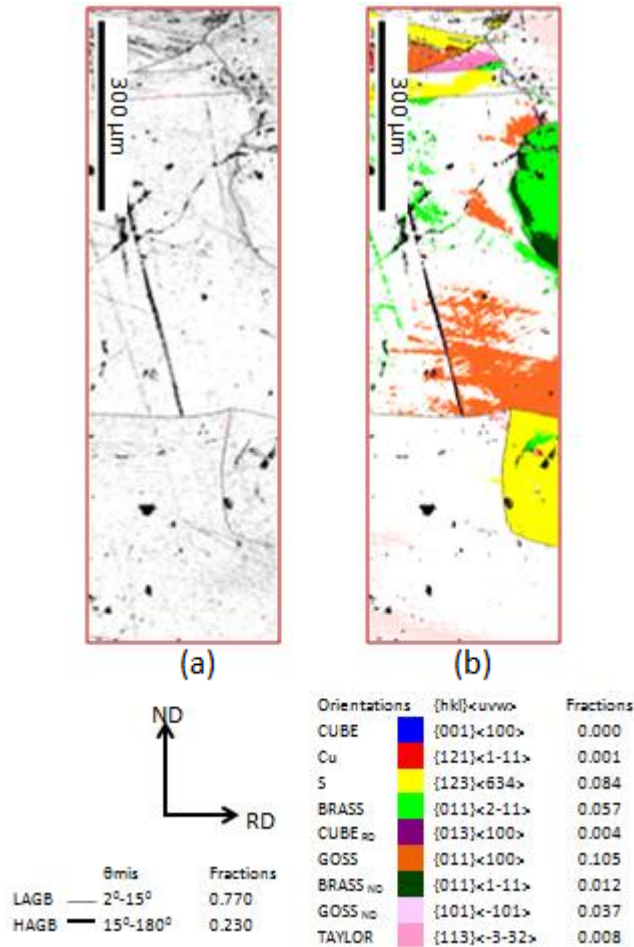


Fig.4.3.1: (a) GB and (b) GO maps of 40% deformed CCR processed material

Figure 4.3.1(a) shows the GB map of the 40% CCR processed material. The structure is characterized rather and similar to the structure observed in the case of UCR processed material at the same deformation level. The fraction of LAGBs increases as compared to the 20% CCR material. Fig.4.3.1 (b) shows the GO map of 40% CCR processed material. It shows weak presence of G and very weak presence of the S, Bs and G_{ND}

components. The weak texture in this condition is also revealed by the (111) pole figure (Fig.4.3.2 (a)) and $\Phi_2=0^\circ, 45^\circ$ and 65° sections of the ODFs (Fig.4.3.2 (c)).

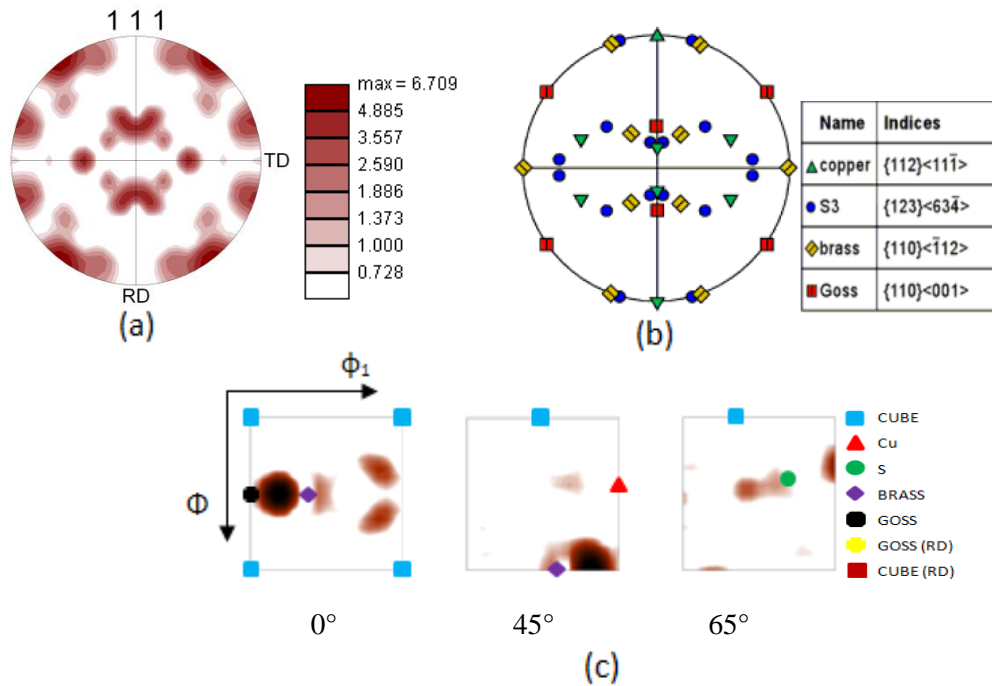


Fig.4.3.2: (a) Experimental (111) pole Figure of 40% deformed CCR processed material and (b) is the ideal (111) pole figure; (c) shows the $\Phi_2=0^\circ, 45^\circ$ and 65° sections of the ODF.

Figure 4.3.3(a) shows the GB map of the 65% CCR processed material revealing the banded and elongated structure. LAGBs inclined to the RD could also be observed here as like its UCR processed counterpart. The inter-band spacing is more than $100\mu\text{m}$ which indicates that the microstructure in this condition is still fairly coarse. The adjacent bands appear to belong to different orientations as may be seen from the corresponding GO map (Fig.4.3.3 (a)). The presence of the S, B_s and G oriented bands as observed in the GO map is clearly evidenced from the (111) pole figure (Fig.4.3.4(a)) and the $\Phi_2=0^\circ, 45^\circ$ and 65° sections of the ODF (Fig.4.3.4(b)) for this deformed condition.

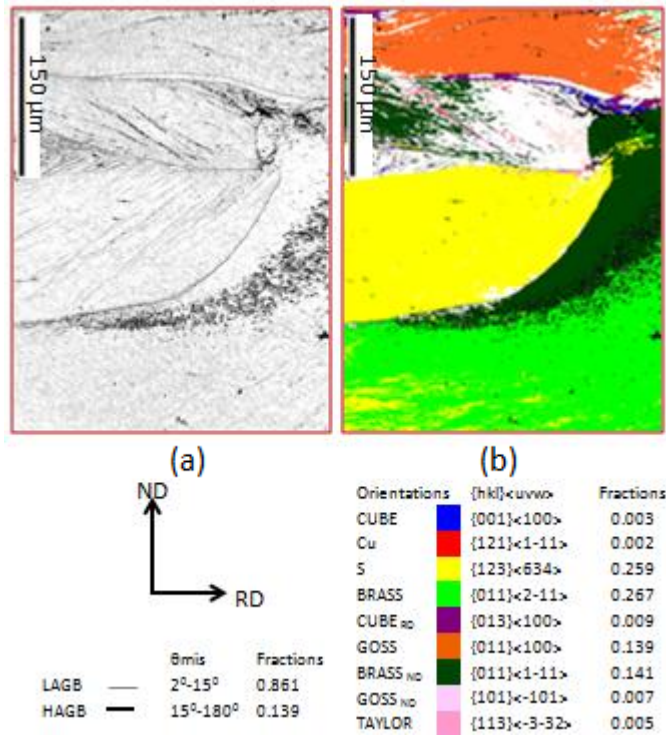


Fig.4.3.3: (a) GB and (b) GO maps of 65% deformed CCR processed material

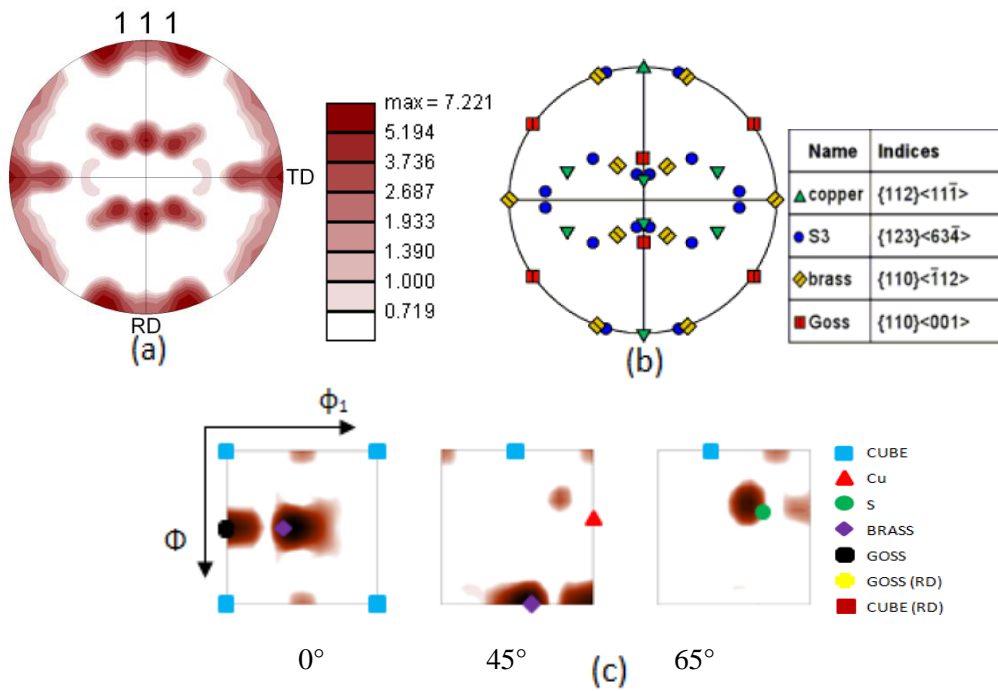


Fig.4.3.4: (a) Experimental (111) pole Figure of 65% deformed CCR processed material and (b) is the ideal (111) pole figure; (c) shows the $\Phi_2=0^\circ, 45^\circ$ and 65° sections of the ODF.

Figure 4.3.5 (a) shows the GB map of a region of interest in 90% CCR processed material. The microstructure is fragmented and wavy having the features associated with local shearing. The GO map (4.3.5(b)) indicates the presence of fragmented and scattered S and B_S oriented regions. The dominant texture component in this condition is S having a volume fraction of ~36% followed by the B_S component (15%). It may be noted that the presence of other texture components including the B_S^{ND} component is rather insignificant in this region. Presence of S and B_S component is also quite easily observed in the corresponding pole figure (Fig.4.3.6 (a)) and ODF (Fig.4.3.6 (b)) section.

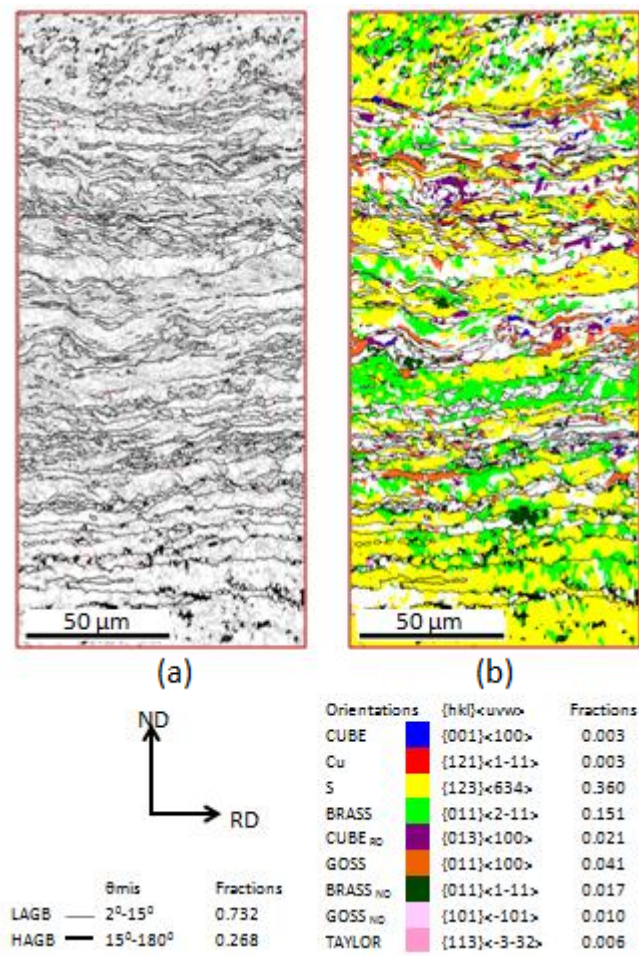


Fig.4.3.5: (a) GB and (b) GO maps of 90% deformed CCR processed material

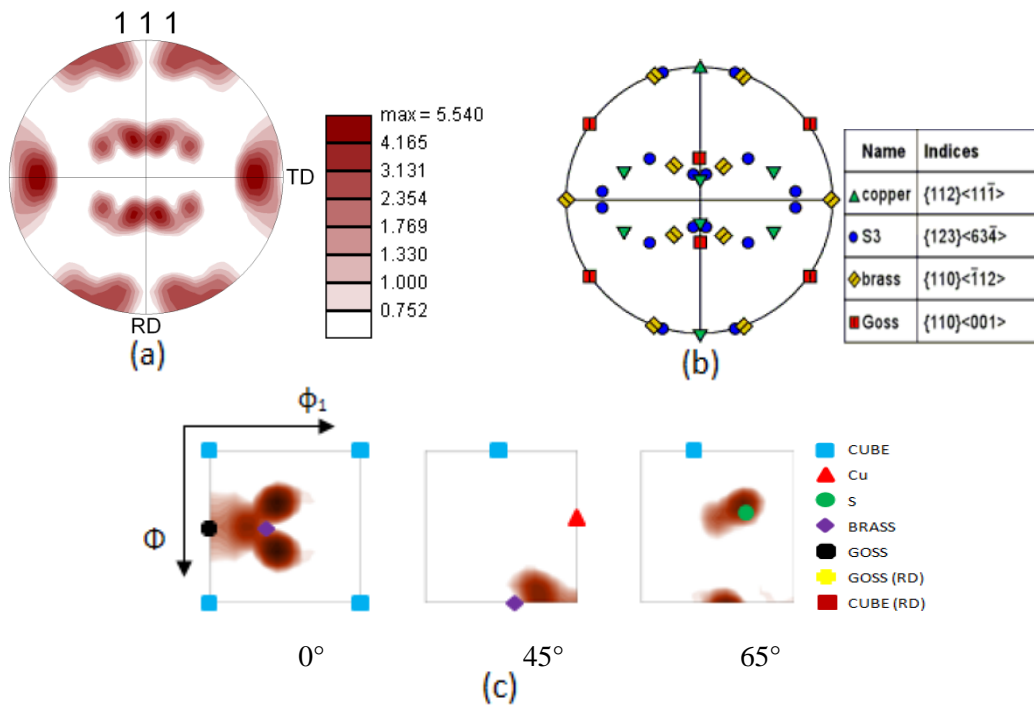


Fig.4.3.6: (a) Experimental (111) pole Figure of 90% deformed CCR processed material and (b) the ideal (111) pole figure; (c) shows the $\Phi_2=0^\circ, 45^\circ$ and 65° sections of the ODF.

The evolution of deformation texture by CCR processing has been further analyzed by XRD. Fig.4.3.7 (a), 4.3.7(b) and 4.3.7 (c) shows the (111) pole figure, standard pole figure and the ODF, respectively, of the 90% CCR processed material. A comparison of the pole figure with the ideal (111) pole figure, shown previously, would clearly reveal that strong intensities are found around the S orientation. The $\Phi_2=0^\circ$ section shows the presence of G component but no significant presence of the B_S component. The $\Phi_2=45^\circ$ section also show the presence of Cu but absence of any strong B_S component. The $\Phi_2=65^\circ$ section reveals the presence of very strong S component in the 90% deformed CCR processed material. Thus, the bulk texture results agree quite well with the microtexture observations and both the experimental measurements do not indicate any significant presence of B_S or B_S^{ND} component.

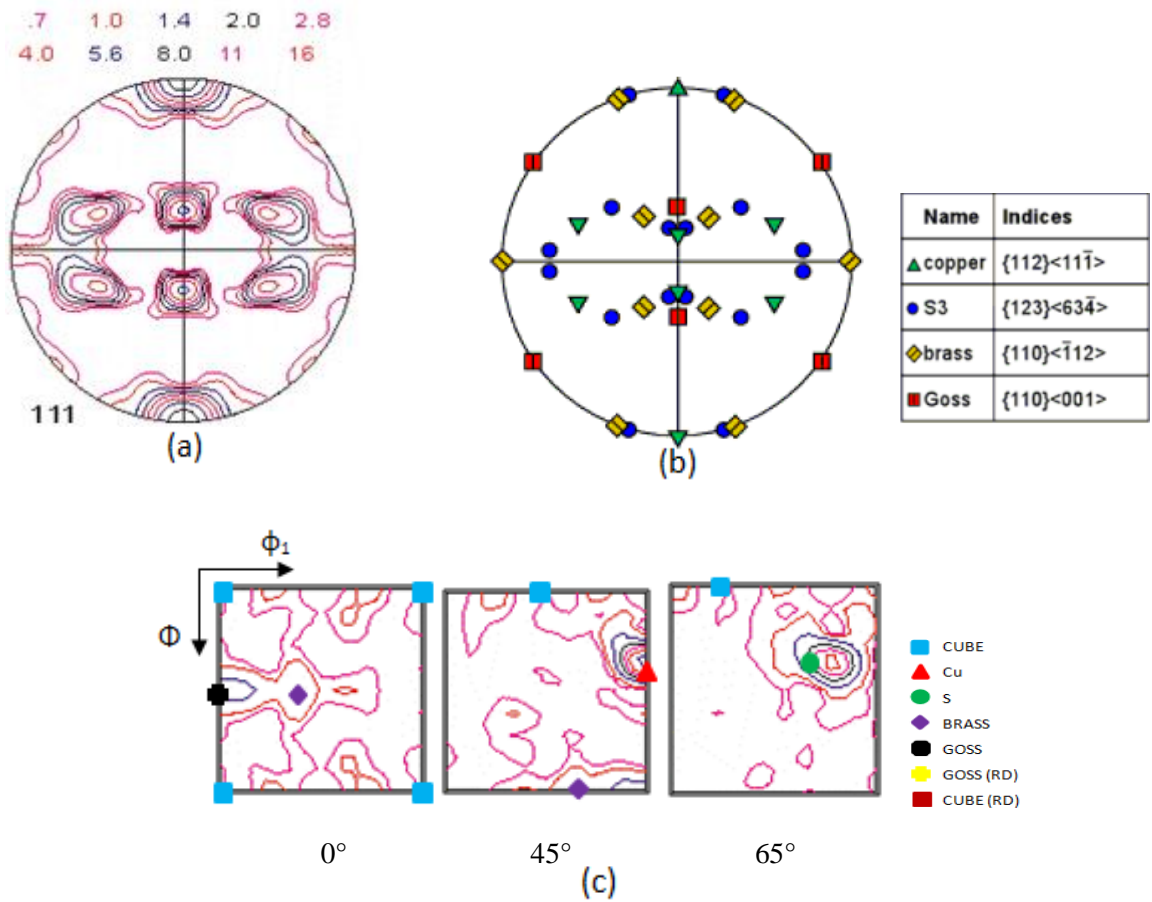


Fig.4.3.7: (a) Experimental (111) pole Figure of 90% CCR processed material and (b) is the ideal (111) pole figure; (c) shows the $\Phi_2=0^\circ, 45^\circ$ and 65° sections of the ODF. All measurements are obtained by XRD.

4.4 Evolution of Mechanical Properties

The evolution mechanical properties during two processing routes were evaluated by hardness testing as shown in Fig. (4.4), hardness of UCR material consistently increases with increasing deformation. However, in the case of the CCR processed material initially it increases up to 65% deformation and then the hardness is found to decrease following 90% deformation.

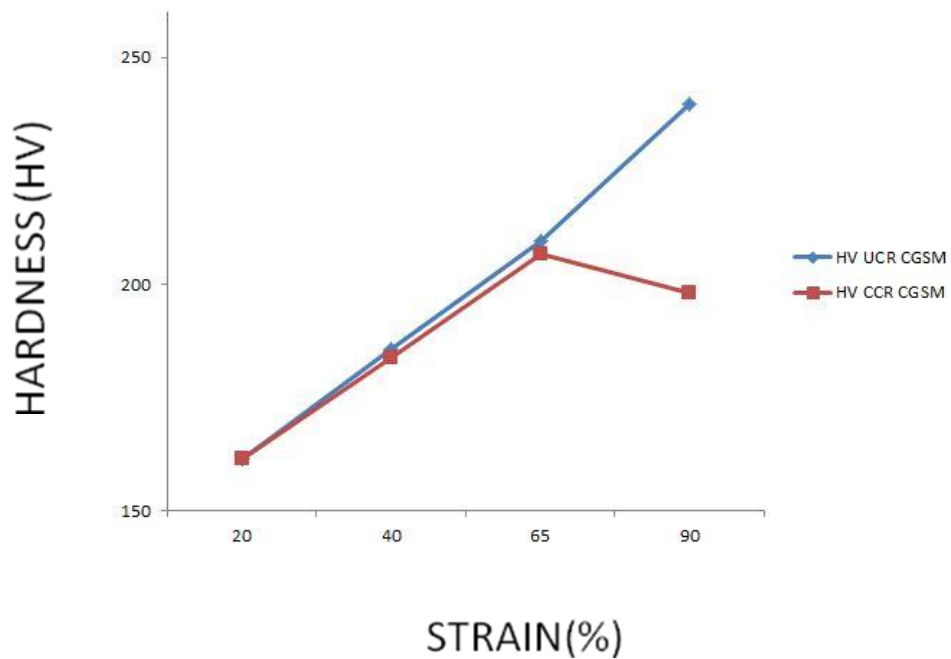


Figure (4.4) - Microhardness Vs Strain plot with increasing strain.

Chapter 5

Discussion

The main observations emanating from this study concerning the microstructure and texture development are that very coarse grained nickel develops a mixture of fragmented and lamellar microstructure and a pure metal type deformation texture characterized by the strong presence of S, B_S and Cu components on the global scale. The texture of CCR processed material is mainly dominated by strong S component. Microtextural heterogeneities can still exist in both cases presumably due to the large starting grain size.

These results differ quite drastically when compared with the results of CCR processed conventional grain sized material. A parallel study carried out at IIT Hyderabad [15] indicates that in conventional grain sized material the CCR processing routes result in a deformation texture is dominated by B_S and B_S^{ND} . However, the UCR processing route yields very similar deformation texture i.e. pure metal or copper type deformation texture irrespective of starting grain size which agrees quite well with previous published results [13, 16]. A comparison presented in Fig. 5.1 clearly elucidates these differences in evolution of deformation texture during CCR processing depending up on the grain size. Previous studies by other authors in CCR processed conventional grain sized Ni and Cu [1, 8] also have reported development of strong B_S and B_S related components. The present study thus points to a very remarkable effect of starting grain size on texture development during CCR processing as compared to the UCR processing. In turn, the CCR processing has much pronounced effect on texture development in conventional grain sized materials as opposed to very coarse grained materials.

The texture development during deformation processing depends critically on the stability of different orientations which may be understood from the rotation rate and divergence rate of different orientations. The rotation rate and divergence calculations of different texture components indicates that stable orientations in the UCR route are the usual cube, Goss, Cu and B_S orientations. During CCR processing of the conventional grain sized material, grains with orientation along the α -fiber will rotate to the B_S orientation and then will rotate further to the B_S^{ND} orientation when the direction of rolling is changed by 90° around the ND, thus, oscillating between the B_S and B_S^{ND} which would be the dynamical end orientations in CCR [1]. In contrast, weaker B_S and B_S^{ND} components in the CCR

processed coarse grained material indicates that the above scheme of crystal rotation may not be true in case of very coarse grained material.

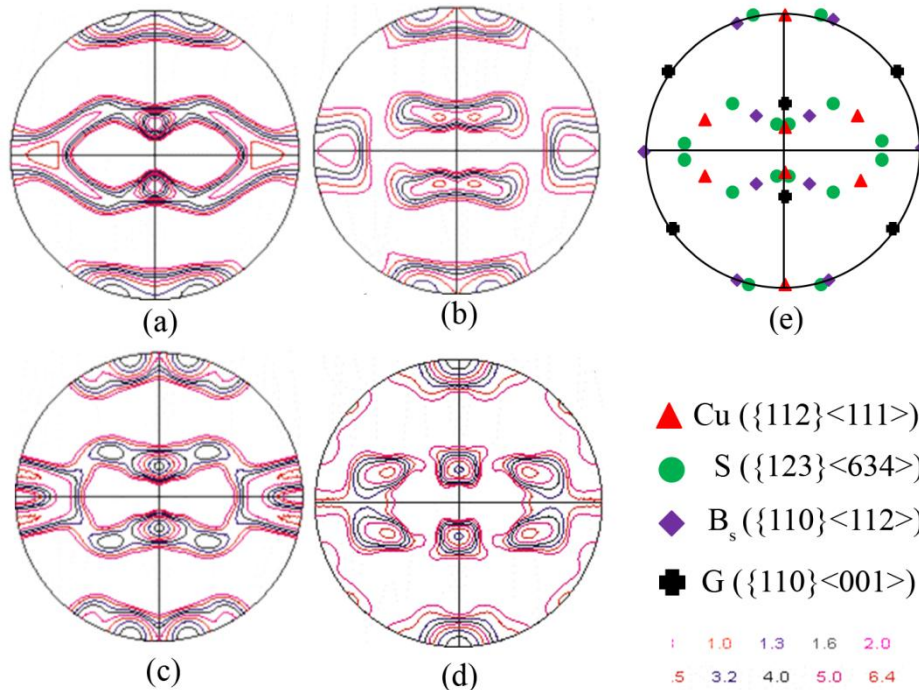


Fig. 5.1: (111) PFs of conventional ((a)-(b)) [1] and coarse grain sized nickel ((c)-(d)) processed by the UCR ((a) and (c)) and CCR ((b)-(d)) routes; Ideal locations of various rolling texture components are shown in (111) PF in (e).

One argument that may be put forward to explain the observed differences is different grain sub-division process, such as, increased propensity for deformation banding in very coarse grain sized materials as compared to conventional grain sized materials. However, this appears to be less likely the reason for the observed differences in the present case as one may always argue that in such a scenario the texture of UCR processed coarse and conventional grain sized materials should also be markedly different. However, the texture of the UCR processed coarse and fine grain sized material appear pure metal or copper type and quite similar as established by bulk texture analysis and also supported by previous studies. Thus, other microstructural reasons should be considered.

One possible reason that might be interesting to consider at this stage would be the effect of local shearing on texture evolution in CCR processed coarse grain sized material. Existence of such local shearing is manifested by wavy and fragmented microstructure of

the CCR processed material. Propensity of local shearing and shear band formation has been reported in very coarse grained materials during cold rolling [13]. Local shearing may result in the fragmentation of structure and rotation of crystals into different orientations and could greatly affect the microtexture development. Support for this observation in the present case might be obtained from the orientation map of CCR processed conventional and coarse grain sized materials. Fragmented B_s oriented regions and random orientations could be found at the vicinity of locally sheared regions (indicated by arrows in the Fig.5.2 (b)) while the local shearing appears to be much weaker in the conventional grain sized material. It appears that due to the local shearing effect the original B_s oriented band, which otherwise might have rotated to the B_s^{ND} orientation, have been fragmented and a part of it has been rotated to assume random orientations.

The evolution of hardness properties in the two processing routes also differ quite significantly. The UCR processed material shows increasing hardness with imposed strain which is clearly explained by the usual strain-hardening phenomenon. Remarkably, the hardness of CCR processed material shows rather unexpected behavior i.e. it first increases up to 65% deformation (due to strain hardening) and then decreases significantly following 90% deformation. Although, the reasons for this behavior remains unclear it may be noted that this drop in hardness also coincides with regime of enhanced propensity for local shearing. However, further studies, including tensile testing are needed to be carried out to clarify the structure-property relationship in CCR processed coarse grain sized material.

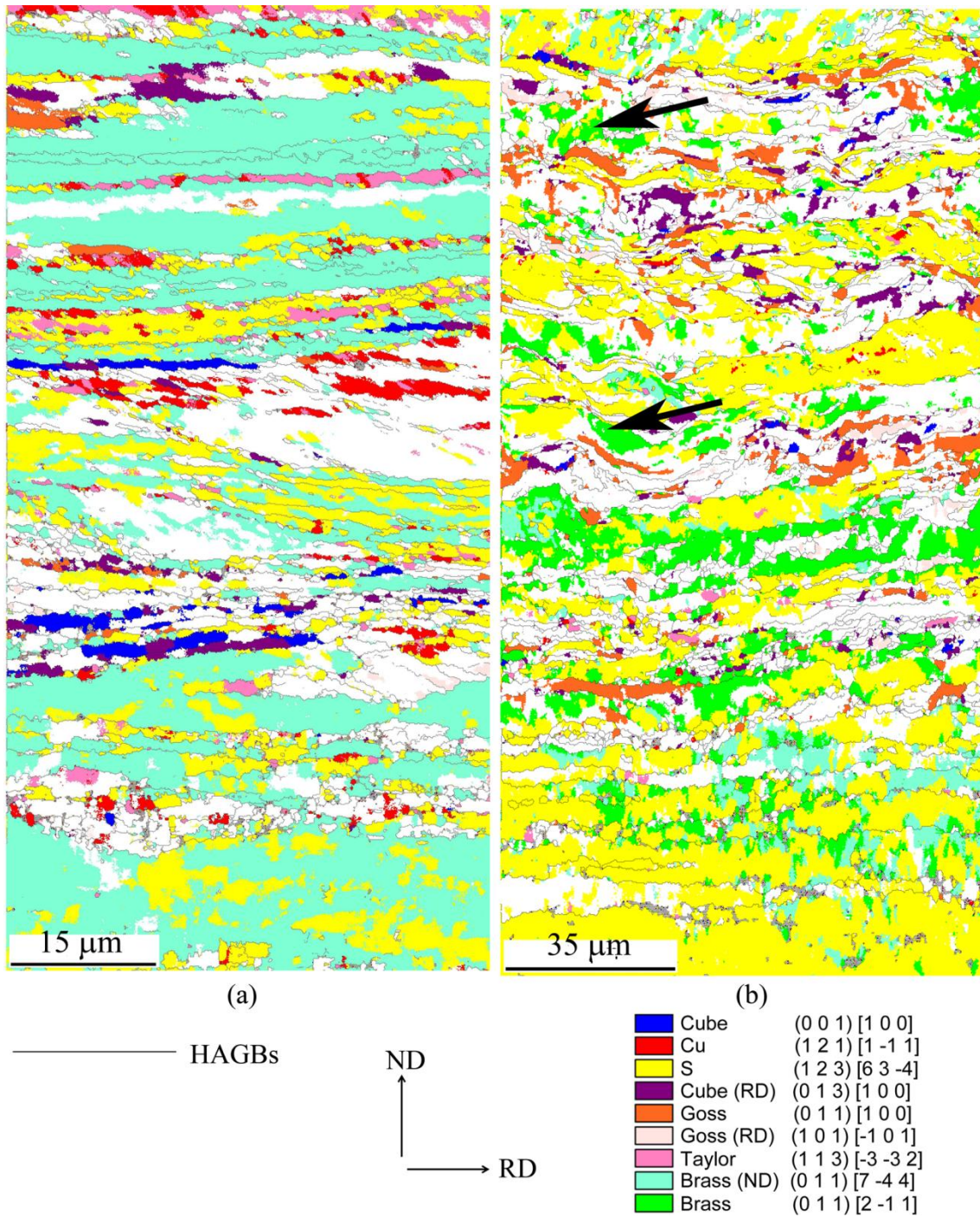


Fig.5.2: GO maps of CCR processed (a) conventional and (b) coarse grain sized materials.

Chapter 6

Summary and Conclusions

High purity nickel with very coarse starting grain sized have been deformed by UCR and CCR processing routes and microstructure and texture of the processed materials have been studied at different length scales using XRD and EBSD. The following conclusions may be drawn from the present study:

1. UCR processing route results in a microstructure having both lamellar and highly fragmented regions. The texture of UCR processed materials may be classified as pure metal or copper type having strong presence of S, Cu and B_S orientations.
2. CCR processing also results in a fragmented microstructure characterized by the presence of locally sheared regions. The micro and global texture of CCR processed materials show strong presence of the S orientation.
3. A comparison with results obtained on conventional grain sized material shows that UCR processing irrespective of grain size results in similar deformation texture in both conventional and coarse grain sized materials. On the other hand, starting grain size has a very strong effect on the evolution of texture during CCR processing.
4. The absence of strong B_S component in coarse grained nickel in contrast to the evolution of strong B_S and B_S^{ND} components in conventional grain sized nickel indicates that scheme of crystal rotation during CCR processing might be different depending on the grain size.
5. Local shearing observed in the microstructure of CCR processed coarse grained material might result in fragmentation of structure and rotation of crystals into different orientation. Fragmented B_S and random orientations at the vicinity of locally sheared regions of CCR processed coarse grained nickel indicates to the important role played by local shearing.

The two different processing routes also show differences in the evolution of hardness properties in coarse grained nickel. The structure-property relationship in CCR processed coarse grained nickel is required to be understand in detail to clarify these differences.

References

- [1] S.H. Hong and D.N. Lee. Deformation and recrystallization textures in cross-rolled copper sheet. *Journal of Engineering Materials and Technology* 124.1, (2002) 13-22.
- [2] S. Suwas and A.K. Singh. Role of strain path change in texture development. *Materials Science and Engineering A* 356(1-2), (2003) 368-371.
- [3] R. E. Bauer. Rudolf, Heinrich Mecking, and Kurt Lücke. Textures of copper single crystals after rolling at room temperature. *Materials Science and Engineering* 27.2, (1977) 163-180.
- [4] J. Hirsch, K. Lücke, and M. Hatherly. Overview No. 76. Mechanism of deformation and development of rolling textures in polycrystalline f.c.c. Metals-III. The influence of slip inhomogenities and twinning. *Acta Metallurgica* 36.11, (1988) 2905-2927.
- [5] J. Hirsch and K. Lücke. Overview no. 76. Mechanism of deformation and development of rolling textures in polycrystalline f.c.c. metals-I. Description of rolling texture development in homogeneous CuZn alloys. *Acta Metallurgica* 36.11, (1988) 2863-2882.
- [6] R. K. Ray. Rolling textures of pure nickel, nickel-iron and nickel-cobalt alloys. *Acta Metallurgica Et Materialia* 43.10, (1995) 3861-3872.
- [7] T. Leffers and R. K. Ray. The brass-type texture and its deviation from the copper-type texture. *Progress in Materials Science* 54.3, (2009) 351-396.
- [8] N. P. Gurao, S. Sethuraman and Satyam Suwas. Effect of strain path change on the evolution of texture and microstructure during rolling of copper and nickel. *Materials Science and Engineering A* 528.25–26, (2011) 7739-7750.
- [9] T. Ozturk. Deformation and recrystallization textures in cross rolled sheets of copper and alpha Brass. *Scripta Metallurgica* 22.4, (1988) 1611-1616.
- [10] T. O. Suet, W. B. Lee and B. Ralph. Deformation and recrystallization in cross- rolled Al-Cu precipitation alloys. *Journal of Materials Science* 29, (1994) 269-275.
- [11] A.A. Ridha and W. B. Hutchinson. Recrystallization mechanisms and the origin of cube texture in copper. *Acta Metallurgica* 30.10, (1982) 1929-1939
- [12] M. Sindel, G. D. Köhlhoff, K. Lücke, and B. J. Duggan. Development of Cube Texture in Coarse Grained Copper. *Textures and Microstructures* 12.1-3, (1990) 37-46.

- [13] P.P. Bhattacharjee, N. Tsuji and R.K. Ray. Effect of initial grain size on the evolution of {001} <100> texture in severely deformed and annealed high purity Nickel. Metallurgical and Materials Transactions A, 42 (2011) 2769-2780.
- [14] S. Y. Han, R. L. Higginson and E.J. Palmiere. The Effect of Grain size and Rolling Reduction on the Texture Development of a Metastable Austenitic Steel. Material Science Forum 558-559, (2007) 195-200.
- [15] M. Joshi. M. Tech. Dissertation, 2012, IIT Hyderabad, India.
- [16] Makita H, Hanada S, Izumi O. Recrystallization in cold-rolled pure nickel. Acta Metall 36, (2011) 403–12